Electronic Supplementary Material (ESI) for Nanoscale.

Supporting Information

The Delicate Balance of Phase Speciation in Bimetallic Nickel Cobalt Nanoparticles

Alberto Palazzolo,[1] Cyprien Poucin,[1] Alexy P. Freitas,[1] Anthony Ropp,[1] Corinne Bouillet,[2] Ovidiu Ersen,[2] Sophie Carenco,[1,]*

[1] Sorbonne Université, CNRS, Collège de France, Laboratoire de Chimie de la Matière Condensée de Paris, 4 place Jussieu, 75005 Paris, France

[2] Institut de Physique et Chimie des Matériaux de Strasbourg (IPCMS), UMR 7504 CNRS−Université de Strasbourg, 23 rue du Loess, BP 43, Strasbourg Cedex 2, France

E-mail: sophie.carenco@sorbonne-universite.fr

Table of contents

1. Reagent and general informations

Oleylamine (OAm; 98%) was purchased from Sigma-Aldrich. Tri-n-octylphosphine (TOP; 97%), dicobalt(0) octacarbonyl ($Co_2(CO)_8$; >95%), and nickel(II) acetylacetonate ($Ni(acac)_2$; anhydrous, min. 95%) were purchased from Strem Chemicals and stored in a glovebox. All chemicals described above were used without further purification. Glassware was kept in an oven at 120 °C prior to utilization.

2. General procedure for the synthesis of NiCo Nanoparticles

A typical synthesis consists of two steps. In a first step, oleylamine (85.8 mmol) is added to a three neck round bottom flask and degassed under vacuum for 15 minutes. $Ni(acac)_2$ (3.9 mmol) and *n*-trioctylphosphine (TOP, 0.8-3 equiv.) are collected in glovebox and added under nitrogen to the flask containing oleylamine. The mixture is rapidly degassed and put under N_2 atmosphere. Thereafter, the mixture is heated up to 215 °C using a heating mantle. After 2 hours, the heating is interrupted and the mixture is cooled down at around 30 °C. In the second step, $Co_2(CO)_8$ is collected in the glovebox and added to the suspension containing Ni NPs under N_2. The mixture is rapidly degassed and put back again under N_2. The reaction is then heated up following the described temperature programs. At the end of the latter, the black magnetic powder is recovered from the flask by using THF and centrifuged three times (9000 rpm, 10 min.) using THF/Ethanol (50/50).

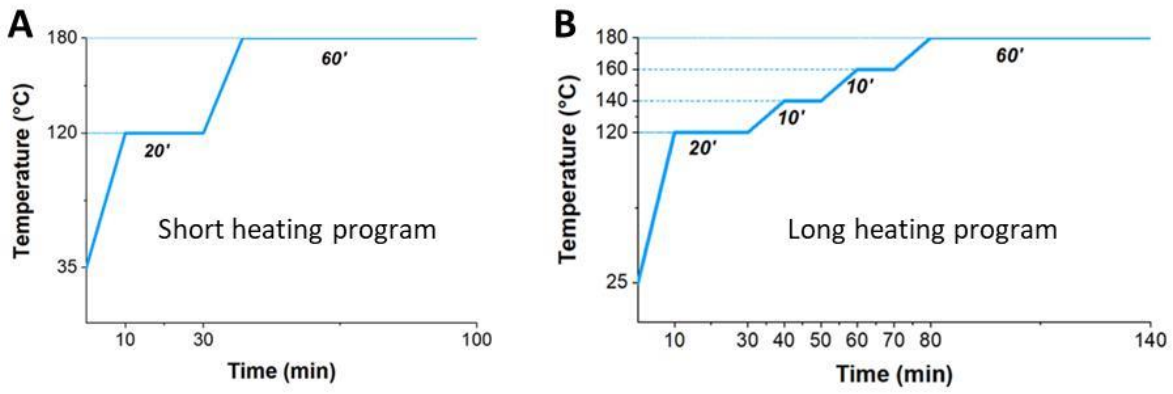

Figure S1 The two heating programs used after the addition of the cobalt precursor. (A) Short heating program with only two plateaus. (B) Long heating program with four plateaus.

3. X-ray diffraction on powder

The different X-ray diffraction patterns of dry powders were measured on a Bruker D8 diffractometer using Cu Kα radiation at 1.5406 Å. Typical diffractograms were collected with a step of 0.05 ° with a scanning speed of 5 s/point. The backgrounds of the diffractograms are subtracted thanks to the EVA software. When low noise Si monocrystals sample holders were used, the angular position 2θ was corrected by adjusting the sample height (correction around 0.5 to 1 mm).

4. Transmission Electron Microscopy and High Resolution TEM

A small quantity of NiCo NPs powder is dispersed in pure THF and allowed to dry on an amorphous carbon coated copper grid.

Low-magnification TEM images were collected with a TWIN 120 (TECNAI SPIRIT) operating at 120 kV with a LaB_6 gun.

HRTEM and low-magnification STEM-EDS spectroscopy was performed on the nanoparticles described in section 2.1 of the article using a JEOL 2100Plus, operating at 200 kV and equipped with a LaB_6 gun. Energy-dispersive X-ray spectroscopy (EDX) characterization was carried out using Oxford, SDD 80 mm2 Xmax with Aztec as software.

STEM bright field (BF), high angle annular dark field (HAADF) images, STEM-EDS and STEM-EELS mapping were acquired using a probe corrector Cs JEOL 2100F microscope operating at 200 kV.

5. Energy Dispersive X-ray spectroscopy

A small amount of powder was deposited on a carbon adhesive tape on a Scanning Electron Microscope sample holder. EDX analyses were performed on a SEM HITACHI S-3400N at 10 kV. Titanium was chosen as reference and analyses were performed on at least three different zones on the sample.

6. X-ray Photoelectron Spectroscopy

X-ray photoelectron spectroscopy was performed on an Omicron Argus X-ray photoelectron spectrometer, using a monochromated Al Kα ($h\nu$ = 1486.6 eV) radiation source having a 300 W electron beam power. The samples were analyzed under ultra-high-vacuum conditions (10^{-8} Pa). After recording a broad range spectrum (pass energy of 100 eV), high-resolution spectra were recorded for the C 1s, Ni+Co 3p core XPS levels (pass energy of 20 eV). The

binding energies were calibrated with respect to the C 1s peak at 284.8eV (adventitious carbon). Spectrum processing was carried out using the CasaXPS software package. The fitting parameters and the color code of the components shown in the XPS spectra are given in the following Table S1. The lineshape was GL(30) for all components. The doublet splittings for Ni 3p and Co 3p were set equal to 1.6 and 1.1 eV respectively.

Table S1 : Fitting parameters for the XPS

Species	B.E. (eV)	FWHM (eV)	Color of the component in the spectra (RGB code)
Ni(0) $3p_{3/2}$	65.2 – 67.5	≤ 5	Dark green (0, 128, 0)
Ni(0) sat.	70.9 – 71.1	≤ 5	Dark green (0, 128, 0)
NiOx $3p_{3/2}$	67.8 – 69.0	≤ 5	Light green (0, 128, 0)
NiOx sat.	72.4 – 72.6	≤ 5	Light green (0, 255, 0)
Co(0) $3p_{3/2}$	59.5 – 60.8	≤ 3	Red (255, 0, 0)
CoOx $3p_{3/2}$	61.0 – 65.0	≤ 5	Deep pink (255, 0, 128)

7. X-ray Absorption Spectroscopy

Nickel K-edge and Cobalt K-edge XAS data were collected on the SAMBA beamline at SOLEIL at an average ring current of 450 mA. 2 mg of the sample was diluted in *ca.* 60 mg of graphite and was compressed to form a 10 mm diameter pellet. Up to nine pellets were fixed with carbon adhesive tape on a sample holder with holes allowing for measurements in transmission mode.

The data for the Co *fcc* reference were provided by Prof. D. Sprouster and previously published in the following article: D. J. Sprouster, R. Giulian, L. L. Araujo, P. Kluth, B. Johannessen, D. J. Cookson, G. J. Foran, M. C. Ridgway, *J. Appl. Phys.* **2010**, *107*, 014313.

8. Intermediate nanoparticles produced with 3 TOP and 12 OAm

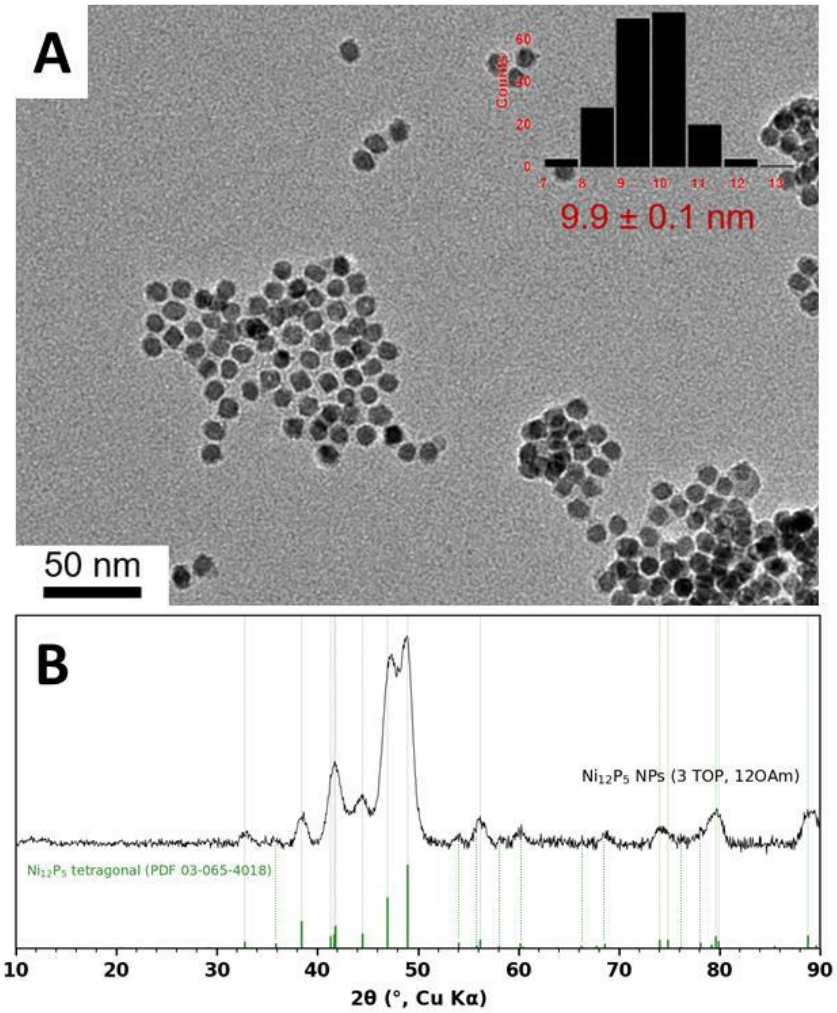

Figure S2 Nanoparticles isolated after the first step of the synthesis with 3 equiv. of TOP and 12 equiv. of OAm, before cobalt addition. (A) TEM observation, size distribution in the inset. (B) XRD pattern (reference phase in green: tetragonal $Ni_{12}P_5$, PDF 03-065-4018). Dotted lines are guide to the eye: these from bottom to top indicate the most intense peaks while these from bottom to the experimental pattern indicate the minor peaks (some of them almost within the experimental noise).

9. Nanoparticles synthetized in concentrated conditions

The synthesis below was performed using 3 equiv. of TOP vs. Ni and 12 equiv. of oleylamine. HRTEM showed poly-crystalline nanoparticles with a number of defects.

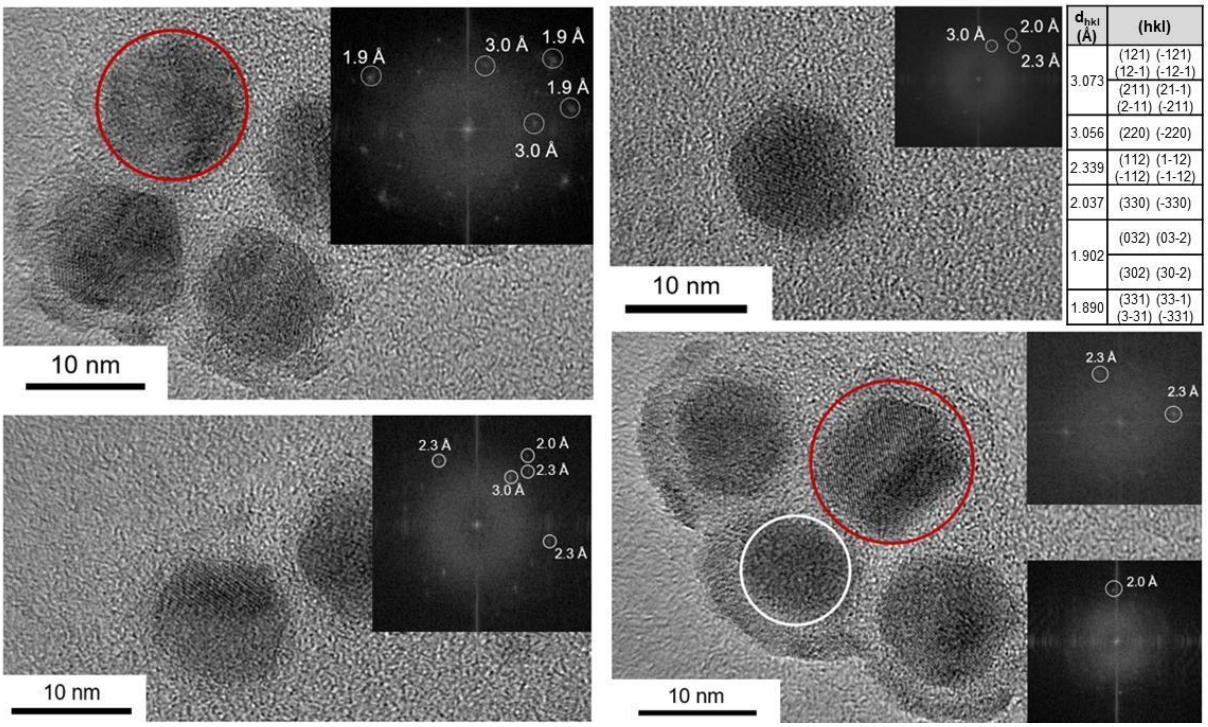

Figure S3 Several HRTEM observations, with, in the inset, the calculated Fast Fourier Transform for selected NPs. Distances are indicated on the insets. A repertory of the corresponding distances expected in the $Ni_{12}P_5$ phase and Miller indexes (ICSD 646121) is on the top right (for simplicity, only the family of planes is indicated, regardless of the direction).

10. Nanoparticles synthesized in diluted conditions with the short heating program

The synthesis below was performed using 3 equiv. of TOP vs. Ni and 22 equiv. of oleylamine.

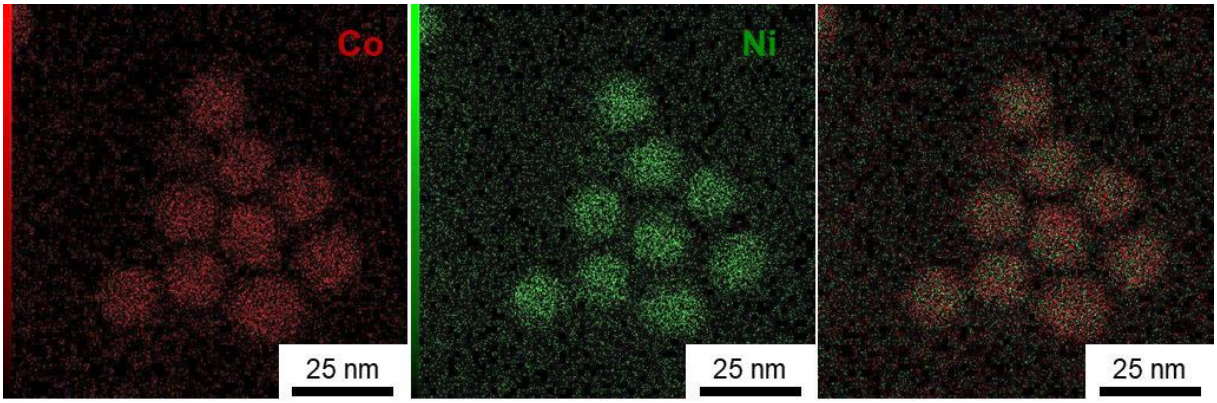

Figure S4 STEM-EDS mapping of the nanoparticles: Co (left), Ni (center) and overlay (right).

The synthesis below was performed using 1 equiv. of TOP vs. Ni and 22 equiv. of oleylamine.

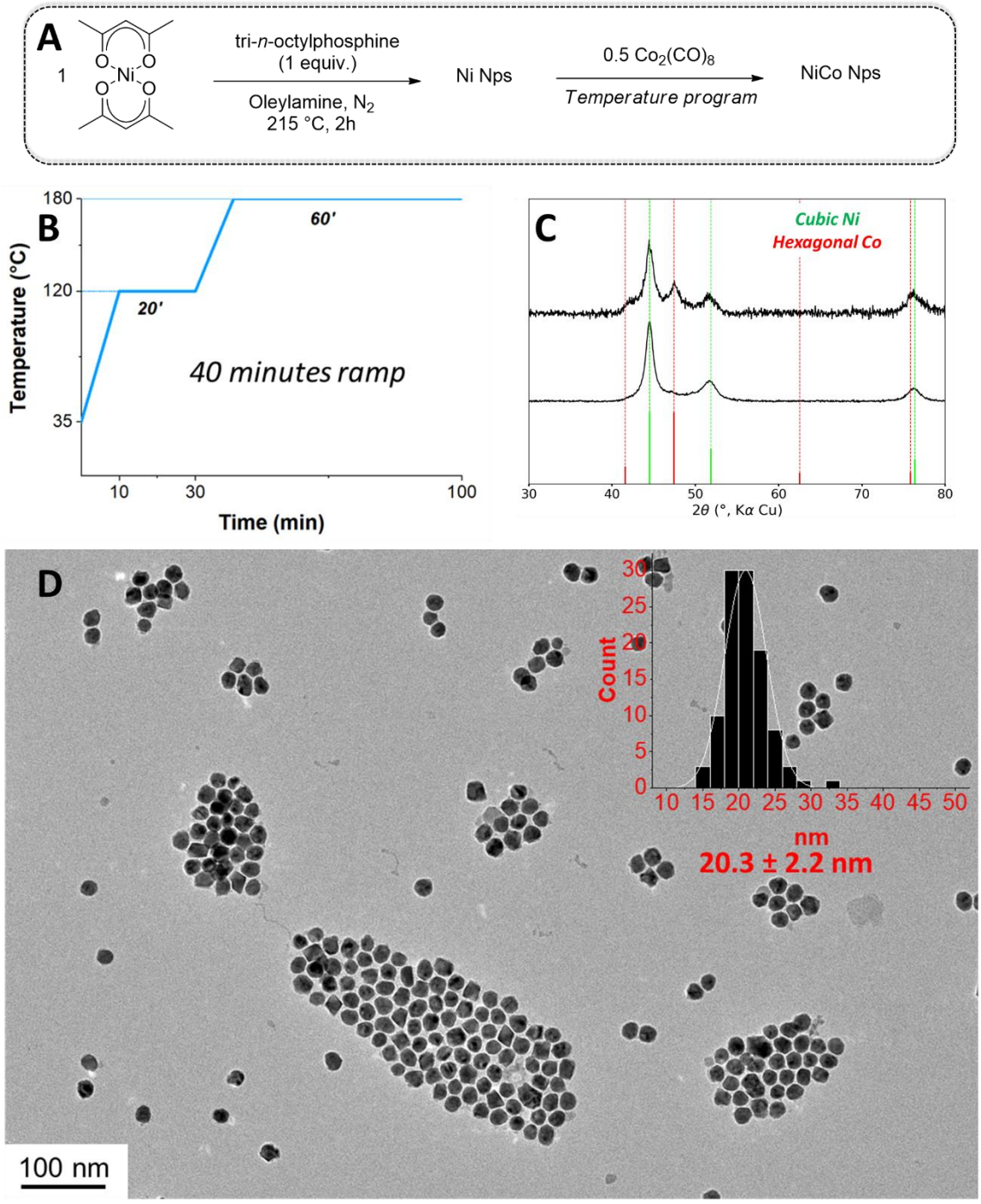

Figure S5 (A) Reaction scheme for the synthesis of NiCo NPs. (B) Temperature program used for the second step, after the addition of the cobalt precursor. (C) XRD patterns from two samples prepared under the same reaction conditions. (D) TEM of the nanoparticles and size distribution in the inset.

The synthesis below was performed using 0.8 equiv. of TOP vs. Ni and 22 equiv. of oleylamine.

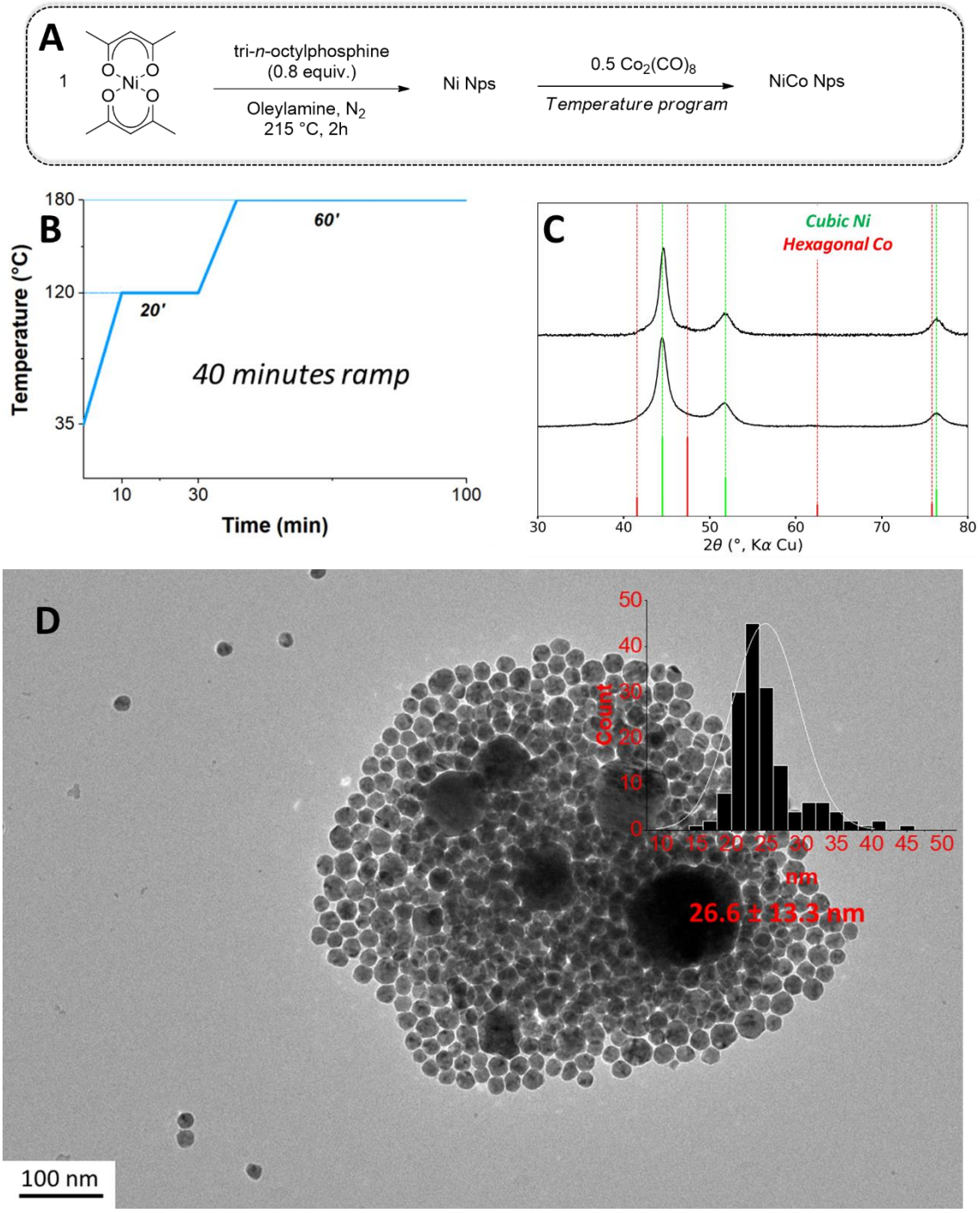

Figure S6 (A) Reaction scheme for the synthesis of NiCo NPs. (B) Temperature program used for the second step, after the addition of the cobalt precursor. (C) XRD patterns from two samples prepared under the same reaction conditions. (D) TEM and size distribution in the inset.

11. Shell thickness of NiCo NPs calculated from a geometrical model

This model assumes that all the Co is deposited on the Ni NPs as a spherical shell.

Let us consider a spherical Ni@Co core-shell nanoparticle with a core radius *R* and a shell thickness *t*. From the definition of density, we get for Ni and Co:

$$\rho_{Ni} = \frac{m}{V} = \frac{M_{Ni} n_{Ni}}{\frac{4}{3}\pi R^3}$$

$$\rho_{Co} = \frac{M_{Co} n_{Co}}{\frac{4}{3}\pi((R+t)^3 - R^3)}$$

From the ratio of the two expressions, we get:

$$\frac{\rho_{Ni}}{\rho_{Co}} = \frac{M_{Ni} n_{Ni}}{M_{Co} n_{Co}} \left(\left(1 + \frac{t}{R}\right)^3 - 1 \right)$$

Let us define α and x:

$$\alpha = \frac{M_{Co} \rho_{\mathrm{Ni}}}{M_{Ni} \rho_{\mathrm{Co}}}$$

$$x = \frac{n_{Co}}{n_{Ni}}$$

We get:

$$\boldsymbol{t = R\left((1 + \alpha x)^{1/3} - 1\right)}$$

And

$$\boldsymbol{x = \frac{1}{\alpha}\left(\left(1 + \frac{t}{R}\right)^3 - 1\right)}$$

The numerical application was done with ρ_{Ni} = 8.908 and ρ_{Co} = 8.850. The atomic radius of cobalt is 135 pm. Starting from Ni NPs of ca 14 nm diameter (as evaluated from Figure S14),

and for x = 0.05, 0.1, 0.2, 0.5, 1, we obtain from our model t = 0.12, 0.23, 0.44, 1.0 and 1.8 nm, respectively.

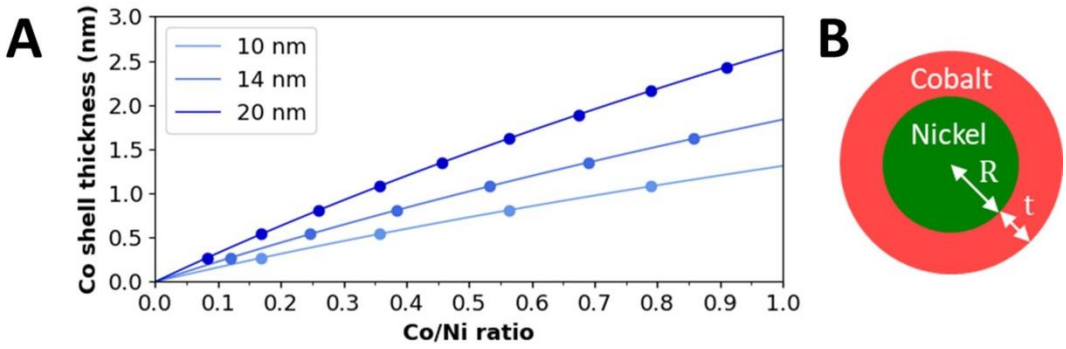

Figure S7 (A) Estimation of the Co shell thickness (t) depending on the Co/Ni ratio and on the initial diameter of Ni NPs. Each dot indicates when a new monolayer can be formed. (B) Scheme of the core-shell NP and the notations used in the calculation.

12. Complementary XAS spectra

XAS spectra of *fcc* NiCo NPs and references:

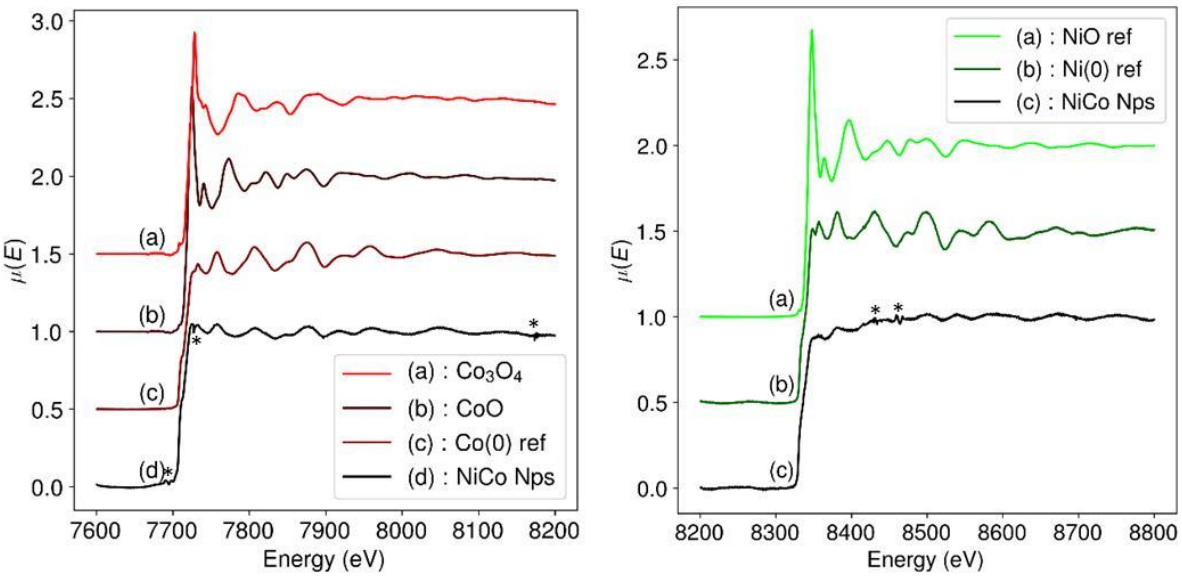

Figure S8 Entire XAS spectra showing a larger part of the EXAFS region of Figure 3, (A) at Co K-edge, (B) at Ni K-edge. *NB*: the small glitches (*) observed on some of the spectra from pellet samples correspond to an imperfect artefact correction related to the use of a monochromator. Perfectly flat and homogeneous samples such as metal foils do not present these glitches.

XANES spectra of nanoparticles prepared with various stoichiometries of cobalt:

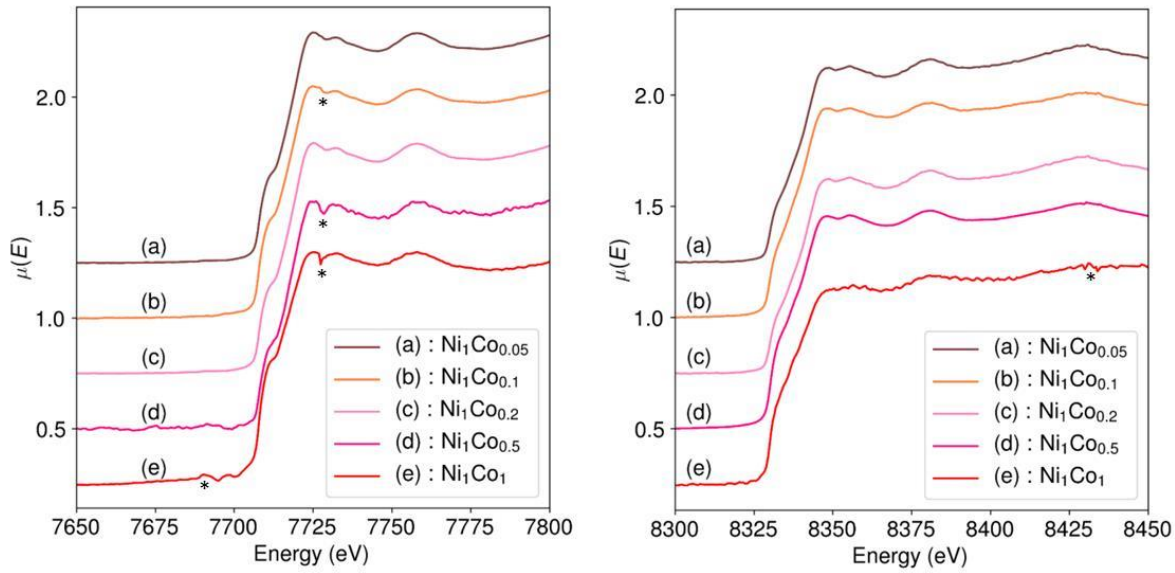

Figure S9 XANES at Co K-edge (left) and Ni K-edge (right) as a function of the number of Co equivalents introduced during the synthesis. *NB*: the small glitches (*) observed on some of the spectra from pellet samples correspond to an imperfect artefact correction related to the use of a monochromator.

13. XRD, TEM and size distribution for NiCo NPs with different ratios of Cobalt

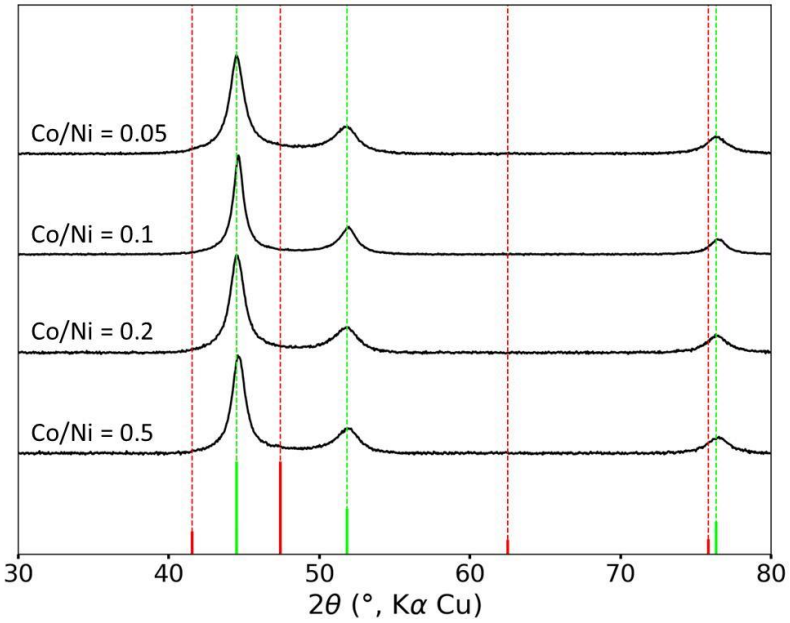

Figure S10 XRD patterns of the samples prepared with various amounts of cobalt. The reference phase in green corresponds to *fcc* Ni, JCPDS file 00-004-0850, and the reference phase in red corresponds to *hcp* cobalt, JCPDS file 04-001-3273.

Table S2 : Average diameters calculated from the population of smaller nanoparticles and for the whole population.

Entry	Ratio Co/Ni	Average diameter of the smaller NPs (10-25 nm) (population in number)	Average diameter of all the NPs
A	0.5	17.5 ± 3 nm (93%)	18.8 ± 6 nm
B	0.2	16.3 ± 2.4 nm (91%)	18.4 ± 7.7 nm
C	0.1	16.2 ± 3 nm (95%)	17.1 ± 6.3 nm
D	0.05	14.4 ± 2 nm (97%)	14.9 ± 4 nm

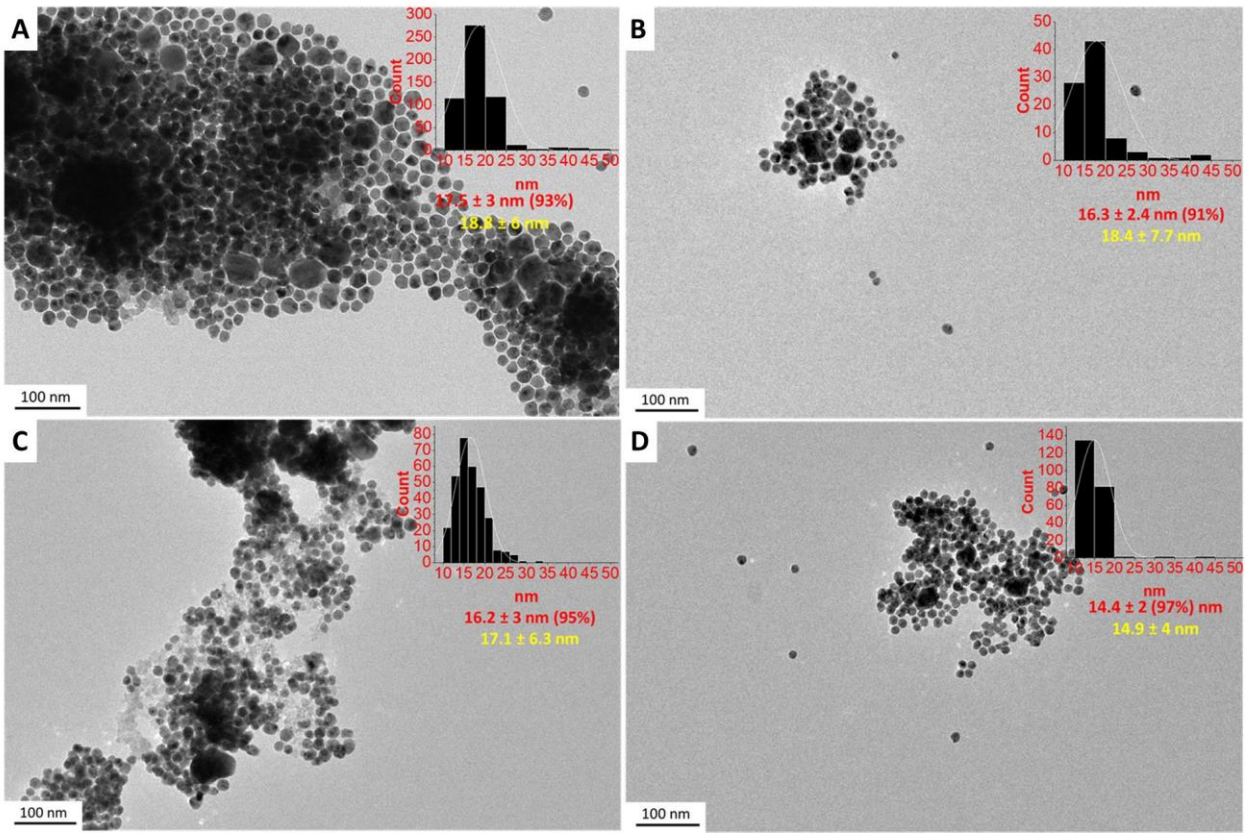

Figure S11 TEM pictures of NiCo NPs with different ratios Co/Ni. (A) Co/Ni = 0.5, (B) Co/Ni = 0.25, (C) Co/Ni = 0.1, (D) Co/Ni = 0.05. The insets show the size distribution. Average diameter in red is for the smaller nanoparticles (10-25 nm) and average diameter in yellow is for the whole population.

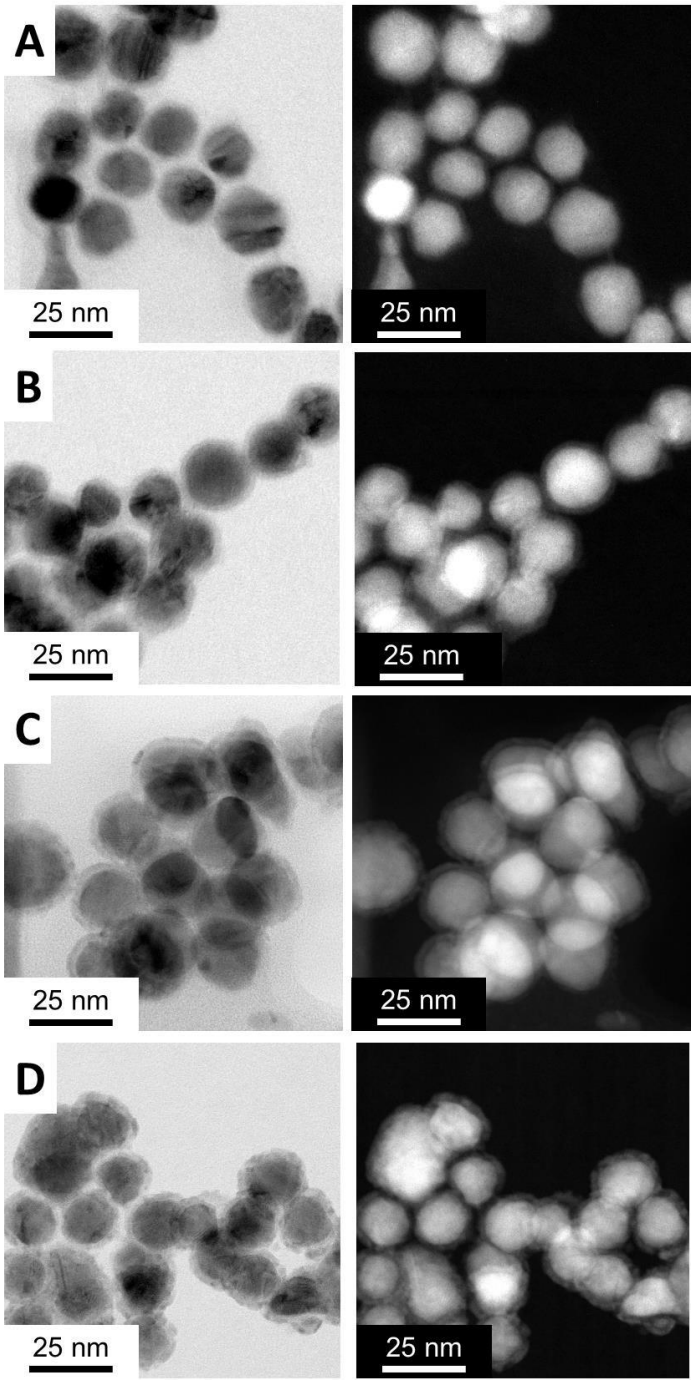

Figure S12 STEM-HAADF pictures, in bright field (left) and dark field (right) modes, of NiCo NPs with different ratios Co/Ni. (A) Co/Ni = 0.5, (B) Co/Ni = 0.25, (C) Co/Ni = 0.1, (D) Co/Ni = 0.05.

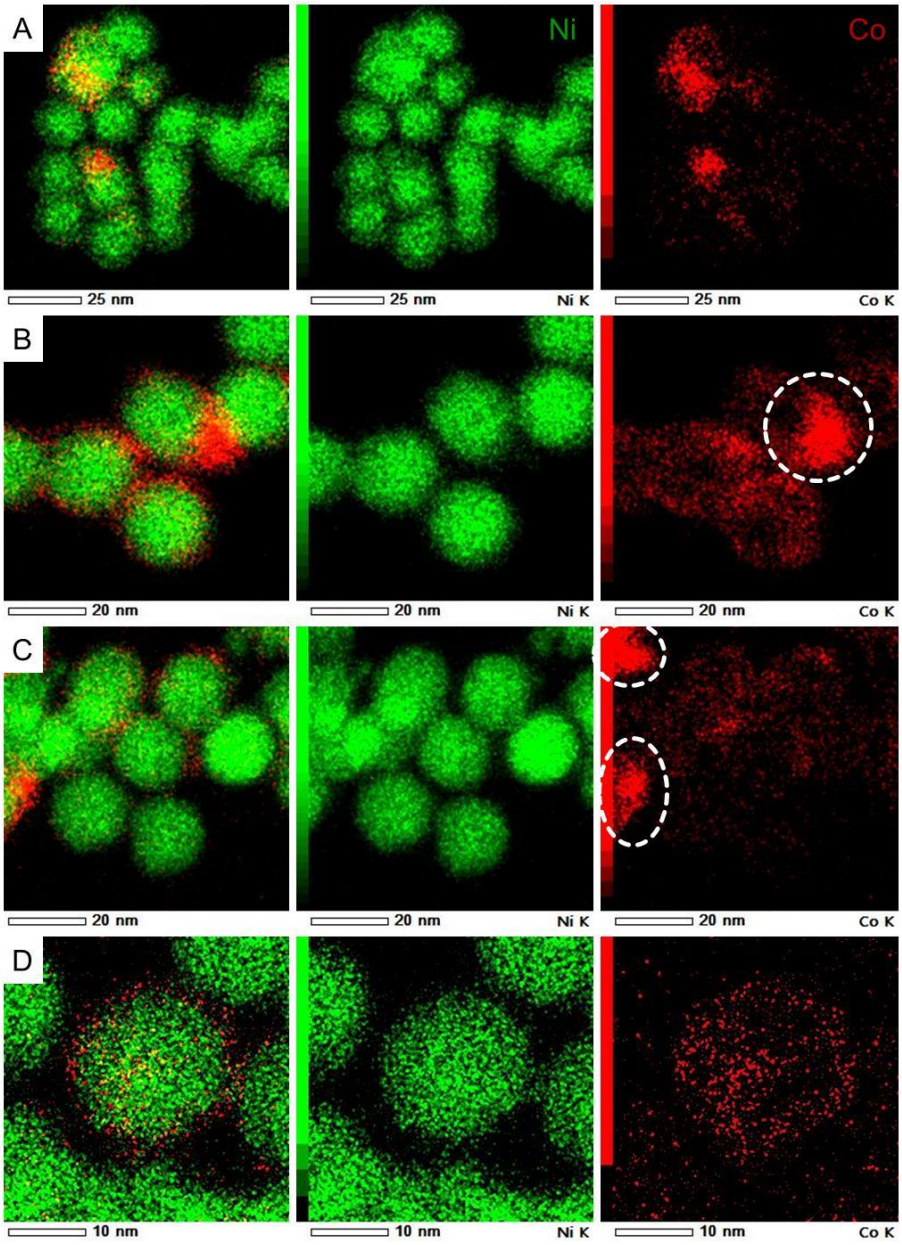

Figure S13 STEM–EDS measurements of NiCo with a variable Co *vs.* Ni ratio. (A) 0.05 (B) 0.1 (C) 0.2 (D) 0.5. From right to left: overlay, nickel and cobalt.

14. TEM of the nanoparticles prior to cobalt precursor addition

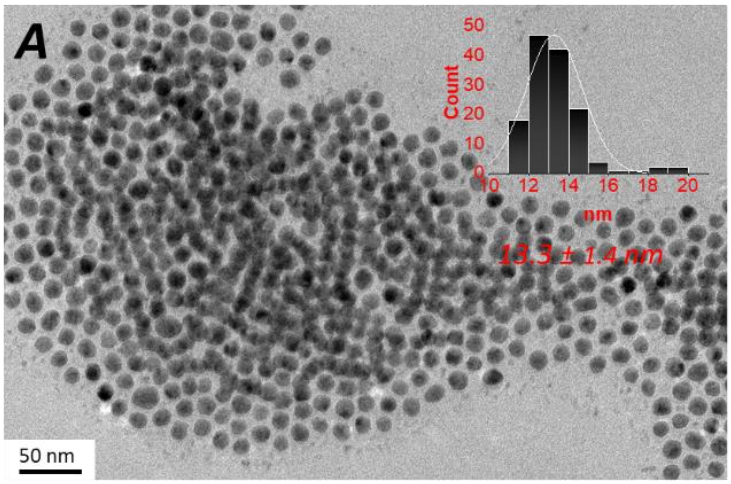

Figure S14 TEM of aliquots collected at the end of the first step of the reaction (before cobalt was added), performed with 22 OAm and 1.0 TOP.

15. ICP-MS and ICP-AES analysis of selected samples

For ICP-AES (Inductively Coupled Plasma-Atomic Emission Spectrometry), we used an Optima 2000 DV (Perkin Elmer) device and for ICP-MS (Inductively Coupled Plasma-Mass Spectrometry) we used a quadrupole ThermoElectron iCAPQ (ThermoFisher Scientific) device. We determined the concentrations in Ni and Co using an external calibration from concentration-certified solutions (SPEX Certiprep). The dilutions are done by weighing in a 2w% ultra-pure aqueous nitric acid solution. The measurements are repeated six times and the mass fractions measured ranged between 0.1 to 1000 ppm. Samples were prepared as follows. For nanopowders resulting of the synthesis (samples ICP1 to ICP5 corresponding to Co/Ni ratio ranging from 1 to 0.05 respectively), 1 mg of powder was dissolved into 10 mL of *aqua regia*. The factors of dilution typically ranged between 1000 to 3000.

Table S3 : ICP-MS and ICP-AES for selected samples

Sample	**Expected Co/Ni ratio**	**Ni conc. (ppm)**		**Co conc. (ppm)**		**Co/Ni ratio**	
		ICP-AES	ICP-MS	ICP-AES	ICP-MS	ICP-AES	ICP-MS
ICP1	**1**	11.6	14.3	11	13.3	**0.95**	**0.93**
ICP2	**0.5**	34.5	43.2	18.4	22.2	**0.53**	**0.51**
ICP3	**0.2**	22.2	32.0	3.4	5.3	**0.15**	**0.17**
ICP4	**0.1**	50.7	73.5	4.9	7.7	**0.10**	**0.11**
ICP5	**0.05**	15.5	24.6	0.6	1.3	**0.04**	**0.05**

16. Analysis of the XRD pattern shown on Figure 2A-(a)

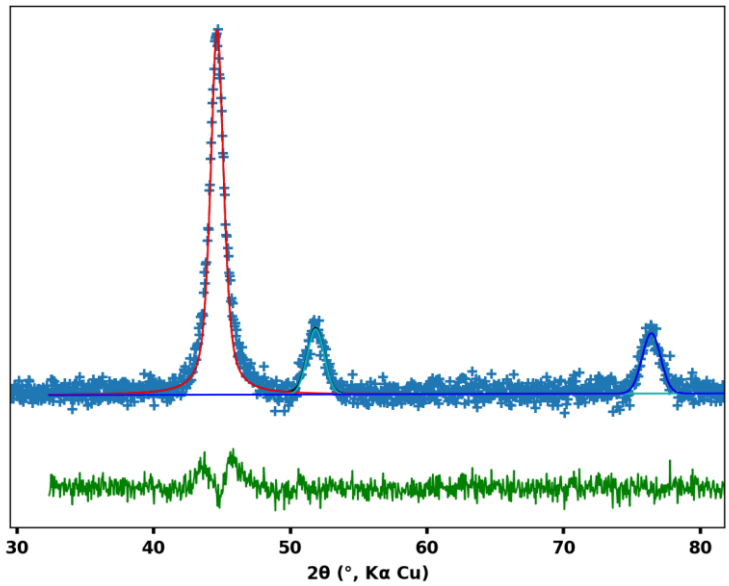

Figure S15 (Top) In blue, experimental XRD pattern. In red, green and deep blue, fitted components. (Bottom) In green, the residue of the fit.